# Accepted Manuscript

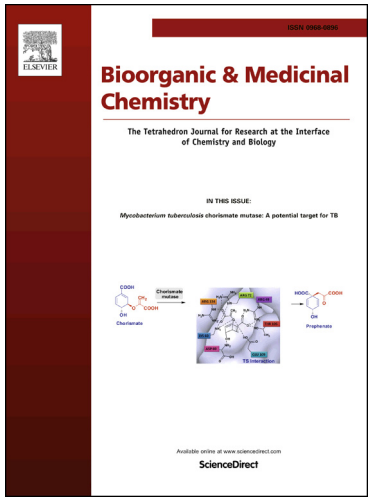


Design and synthesis of bicyclic acetals as Beta Secretase (BACE1) inhibitors

Riccardo Innocenti, Elena Lenci, Gloria Menchi, Alberto Pupi, Andrea Trabocchi

PII: S0968-0896(17)30528-X
DOI: http://dx.doi.org/10.1016/j.bmc.2017.03.030
Reference: BMC 13628

To appear in: *Bioorganic & Medicinal Chemistry*

Received Date: 30 January 2017
Revised Date: 10 March 2017
Accepted Date: 15 March 2017

Please cite this article as: Innocenti, R., Lenci, E., Menchi, G., Pupi, A., Trabocchi, A., Design and synthesis of bicyclic acetals as Beta Secretase (BACE1) inhibitors, *Bioorganic & Medicinal Chemistry* (2017), doi: http://dx.doi.org/10.1016/j.bmc.2017.03.030

## Graphical Abstract

**Design and synthesis of bicyclic acetals as Beta Secretase (BACE1) inhibitors**

Riccardo Innocenti,[a] Elena Lenci,[a] Gloria Menchi,[a,b] Alberto Pupi,[b,c,d] Andrea Trabocchi[a,b,*]

[a] *Department of Chemistry "Ugo Schiff", University of Florence, Via della Lastruccia 13, 50019 Sesto Fiorentino, Florence, Italy*

[b] *Interdepartmental Center for Preclinical Development of Molecular Imaging (CISPIM), University of Florence, Viale Morgagni 85, 50134 Florence, Italy*

[c] *Department of Clinical and Experimental Biomedical Science "Mario Serio", University of Florence, Largo Brambilla 3, 50134 Florence, Italy*

[d] *Azienda Ospedaliera Universitaria Careggi (AOUC), Largo Brambilla 3, 50134 Florence, Italy*

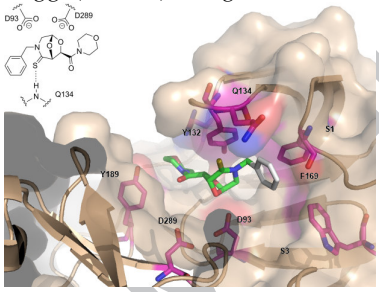

Bioorganic & Medicinal Chemistry
journal homepage: www.elsevier.com

# Design and synthesis of bicyclic acetals as Beta Secretase (BACE1) inhibitors

Riccardo Innocenti,[a,§] Elena Lenci,[a,§] Gloria Menchi,[a,b] Alberto Pupi,[b,c,d] Andrea Trabocchi[a,b,*]

[a] *Department of Chemistry "Ugo Schiff", University of Florence, Via della Lastruccia 13, 50019 Sesto Fiorentino, Florence, Italy*
[b] *Interdepartmental Center for Preclinical Development of Molecular Imaging (CISPIM), University of Florence, Viale Morgagni 85, 50134 Florence, Italy*
[c] *Department of Clinical and Experimental Biomedical Science "Mario Serio", University of Florence, Largo Brambilla 3, 50134 Florence, Italy*
[d] *Azienda Ospedaliera Universitaria Careggi (AOUC), Largo Brambilla 3, 50134 Florence, Italy*

* Corresponding author. Phone, +39 055 4573507; fax, +39 055 4574913; E-mail, andrea.trabocchi@unifi.it.
§ These authors contributed equally to the work.

ARTICLE INFO

*Article history:*
Received
Received in revised form
Accepted
Available online

*Keywords:*
Peptidomimetics
Amino acids
Enzyme inhibition
Alzheimer's disease
Drug discovery

ABSTRACT

Taking advantage of the structural similarity between aspartic proteases, small-molecule peptidomimetic inhibitors that already showed activity towards Secreted Aspartic Protease 2 as anti-Candida agents and HIV protease inhibitors were exploited as potential BACE1 inhibitors. A focused library of 6,8-dioxa-3-azabicyclo[3.2.1]-octane peptidomimetic scaffolds was synthesized and assayed towards BACE1 enzyme, resulting in the identification of a thiolactam-containing hit compound possessing $IC_{50}$ in the low micromolar range, and confirming the bicyclic acetal portion as a potential transition state analogue in the interaction with catalytic aspartic acid residues.



## 1. Introduction

According to the World Health Organization (WHO), about 35.6 millions people have been diagnosed for dementia in 2010, and the number is projected to double every twenty years.[1] The overall cost for dementia worldwide has been estimated approximately 604 billion dollars.[2] Alzheimer's Disease (AD) is the most common cause of dementia in older people, consisting of a chronic and progressive neurodegenerative disorder.[3] The classic clinical symptoms of the disease are memory loss and difficulties with thinking, problem-solving or language. Actually, the accessible therapies for such disease succeeded only in slowing the cognitive decline due to AD. The pathological hallmarks of AD include two types of lesions in the brain, the extracellular accumulation of amyloid plaques composed of the β-amyloid (Aβ) peptide, and intracellular neurofibrillary tangles (NFT) resulting from the aggregation of hyperphosphorylated microtubule-associated protein tau.[4]

The formation of Aβ is a sequential proteolytic process consisting of the cleavage of the amyloid precursor protein (APP) by the β- and γ-secretase enzymes. The β secretase, referred to as *Beta-site Amyloid precursor protein (APP) Cleaving Enzyme 1* (BACE1), is the enzyme that initiates Aβ production by cleaving the extracellular domain of APP, generating a *N*-terminal Aβ fragment and the membrane bound *C*-terminal fragment C99.[5] Successively, intramembrane processing of the latter fragment by γ-secretase yields Aβ.[6] Most Aβ peptides terminate at residue 40 but about 5-10% ends at residue 42, which is a major player in AD pathogenesis. Thus, both β and γ secretases are required for the production of Aβ, and the inhibition or modulation of these enzymes has been considered a key therapeutic approach for reducing cerebral Aβ concentrations in patients with AD. The important role of BACE1 in APP processing was evinced *in vivo* from studies with knockout mice showing that both wild type and mutant forms of APP failed to produce Aβ in the absence of BACE1,[7] further corroborating the importance of BACE1 as a target for the therapeutic intervention of AD.

The first-peptide based BACE1 inhibitors used a transition-state mimetic approach using a non-hydrolyzable peptide isostere at the scissile site. Successively, other non-peptide inhibitors based on diverse heterocyclic scaffolds were developed, all addressing the catalytic aspartic acid diad through acid-base and hydrogen-bond interactions.[8] Some of these molecules possessing high efficacy *in vitro* proved to reduce the secretion of Aβ in cell cultures.[9] Indeed, an important issue in the development of BACE1 inhibitor drugs encompasses the difficulty in crossing the blood-brain barrier (BBB), thus resulting in low potency *in vivo,* and recent papers reported interesting improvements towards brain penetration.[10,11]

Several years ago our research group introduced a novel class of bicyclic peptidomimetic scaffolds showing dipeptide isostere potential.[12] Such compounds are easily achieved from the synthetic combination of suitable amino acids and tartaric acid or

carbohydrates derivatives, and show remarkable stability of the acetal portion to acidic conditions.[13] More recently, we identified this class of peptidomimetic compounds as potential aspartic protease inhibitors taking advantage of their role as dipeptide isosteres, and of the bicyclic acetal portion as a potential transition-state analogue in the interaction with key residues of enzyme's catalytic site. Among this library of peptidomimetics, two hit candidates proved to be effective against drug-resistant *C. albicans* strains in *in vivo* experiments.[14-16] The structural analogy of aspartic proteases expressed in different pathological systems suggested the screening of this library of bicyclic compounds towards other important therapeutic targets, such as the HIV protease. Indeed, sub-micromolar hit compounds were identified as HIV protease inhibitors,[17] thus corroborating the capability of these compounds as aspartic protease inhibitors by means of a transition-state isosterism.

Accordingly, in this work we envisaged the application of these bicyclic compounds against BACE1 as an additional aspartic protease target. The analysis of the similarity of BACE1 with SAP2 from *C. albicans* and HIV-1 protease was carried out through molecular modeling, and the key structural features of the active site were investigated by a three-dimensional structural superimposition of BACE1 with SAP2 and the HIV protease. Also, we expanded the array of this class of bicyclic compounds by the synthesis of novel bicyclic thiolactams, with aim to explore the potential of the sulfur atom as a hydrogen-bond acceptor in the key functional group at position 2 of these scaffolds, and we applied them together with representative library members in enzyme inhibition assays for the identification of novel BACE1 inhibitors.

## 2. Results and Discussion

**3D Structural alignment.** BACE1 is a transmembrane aspartic protease adopting a bilobal structure with the substrate binding pocket between the N-terminal and C-terminal lobes of the enzyme. It is closely related to the pepsin family of aspartic proteases, and the catalytic domain of BACE is characterized by the two canonical aspartic protease motifs of the sequence DTGS and DSGT that both contribute to form the active site of the enzyme.[8,18] The flap region closes over the top of the cleft when bound to the substrate/inhibitor and is characterized by Y132, T133 and Q134.

We investigated the structural similarity between BACE1 and both SAP2 and HIV protease, and the key structural features around the active site characterized by the flap region and the two DTGS and DSGT aspartic protease motifs by a three-dimensional structural superimposition of the proteases using molecular modeling (Figure 1). The Swiss PDB viewer (SPDBV) program (4.0.1 version, Swiss Institute of Bioinformatics)[19,20] was used to superimpose three dimensional (3D) structures of the aspartic proteases taking into account the alpha-carbon atoms of the highly conserved DTG motifs.

The superimposition of the HIV protease (PDB: 4HLA) and BACE1 (PDB: 4J0P) resulted in the optimal alignment of the two canonical aspartic protease motifs of the sequence DTG and DSG, showing a RMSD of 1.48 ang calculated on all alpha-carbon atoms (Figure 1, top). Although the flap regions proved to overlap in general 3D structure, I50 of the HIV protease overlapped with Y132 of BACE1 rather than Q134, which is the corresponding hydrogen-bond donor in BACE1 interacting with the substrate/inhibitor. Accordingly, Q134 proved to be distant from the aspartic protease motifs of about 3.8 ang more than the corresponding I50 as in the HIV protease. Similarly, the superimposition of SAP2 of *C. albicans* (PDB: 1EAG) and BACE1 (PDB: 4J0P) resulted in perfect alignment of the two DTG and DSG aspartic protease motifs, showing a RMSD of 1.44 ang calculated on all alpha-carbon atoms (Figure 1, bottom). Even in this case, the flap regions showed some degree of overlap, although BACE1 showed flap residues being somewhat distant to catalytic aspartic acid residues with respect to SAP2. Specifically, the interactive hydrogen-bond donor Q134 of BACE1 proved to be distant to the DTG/DSG protease motifs by about 3.7 ang more than the corresponding G85 of SAP2, similar to what was observed for the HIV protease. This evidence showed that the 3D structural similarity was not as strict as observed in the case of SAP2/HIV protease overlap,[21] and was considered an important rationale for the selection of candidate bicyclic scaffolds addressing both the catalytic aspartic acids and the flap region for the inhibition assays towards BACE1.

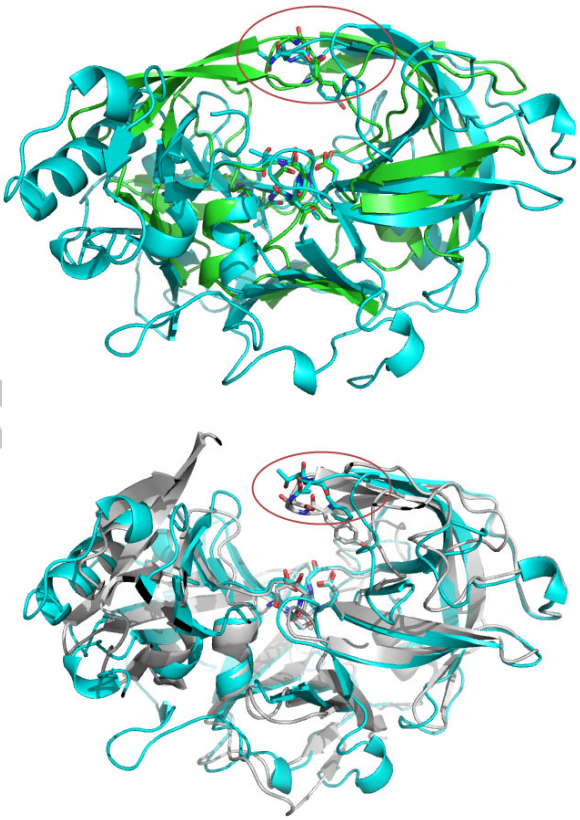

**Fig. 1**. Top: superimposition of HIV-1 protease (PDB: 4HLA in green) and BACE1 (PDB: 4J0P in cyan); down: superimposition of *C.albicans* SAP2 (PDB: 1EAG in grey) and BACE1 (PDB: 4J0P in cyan). Both fittings have been obtained with SPDBV. The red circles highlight the 3D overlap of the aspartic protease residues around the flap regions.

**Pairwise sequence alignment.** Despite differences in both size and overall amino acid sequence between BACE1, SAP2 from *C. albicans*, and the HIV-1 protease, significant homologies exist between their active sites. In order to compare the primary structures of these proteases, we performed a local sequence alignment using the EMBOSS matcher algorithm,[22] and high similarity was found in the active site regions of both SAP2 and the HIV-1 protease (Figure 2 and Table 1). Indeed, sequence alignment of active sites containing the DTG motif disclosed a similarity of 55% and identity of 30% between BACE1 *N*-terminal domain (79-98 residues) and HIV-1 protease active site region (11-30 residues). Higher similarity was found when comparing the *N*-terminal regions of BACE1 (75-101 residues)

and SAP2 (14-40 residues), both containing the DTG sequence, which showed 74.1% of similarity and 55.6% of identity. In addition, the *C*-terminal regions of these two proteases showed some degree of similarity, too, possessing 48.6% of similarity and 18.9% of identity around the DSG catalytic motif.

**Table 1.** Local sequence similarities between BACE1 (4J0P) and SAP2 (1EAG) / HIV-1 aspartic protease (4HLA) in the active site region performed using EMBOSS matcher pairwise sequence alignment.

| Enzymes | Sequence | % identity | % similarity |
|---|---|---|---|
| *N*-terminal BACE1 *vs* HIV pr | 79-98 vs 11-30 | 30 | 55 |
| *N*-terminal BACE1 *vs* SAP2 | 75-101 vs 14-40 | 55.6 | 74.1 |
| *C*-terminal BACE1 *vs* SAP2 | 287-323 vs 215-252 | 18.9 | 48.6 |

```
BACE1 (4J0P)      79  MTVGSPPQTLNILVDTGSSN  98
                      :|:....|....|:|||:.:
HIV pr(4HLA)      11  VTIKIGGQLKEALLDTGADD  30
------------------------------------------------------------
N-terminal
BACE1(4J0P)       75 YYVEMTVGSPPQTLNILVDTGSSNFAV 101
                     |..:::|||..|.||::|||||:..|
SAP2 (1EAG)       14 YAADITVGSNNQKLNVIVDTGSSDLWV 40
------------------------------------------------------------
C-terminal
BACE1(4J0P)      287 IVDSGTTNLRLPKKVFEAAVASIKAASSTEKFPDGFW 323
                     ::|||||...|.:.:.:..:.:.....:.:...:.|:
SAP2 (1EAG)      216 LLDSGTTITYLQQDLADQIIKAFNGKLTQDSNGNSFY 252
```

**Fig. 2**. Sequence alignment between BACE1 (4J0P) and SAP2 (1EAG) / HIV-1 aspartic protease (4HLA) in the active site region using EMBOSS matcher pairwise sequence alignment.

**Synthesis**. The synthesis of bicyclic peptidomimetic compounds was achieved using suitable amino acid and tartaric acid derivatives through a coupling/cyclization approach, as previously reported.[12,13] Moreover, in order to expand the array of bicyclic compounds with scaffold possessing the internal C=S bond, a series thiolactams were conceived and synthesized from the parent esters (Scheme 1).

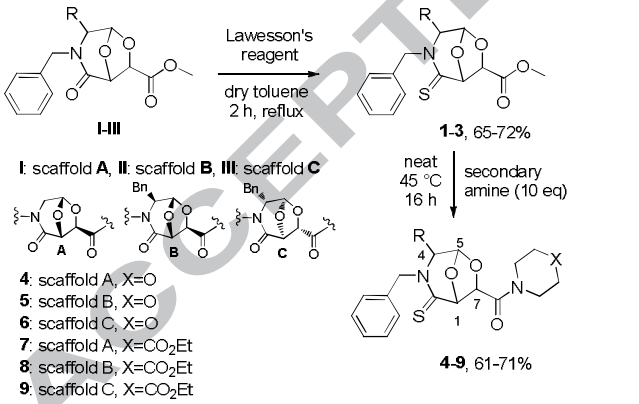


**Scheme 1.** Synthetic approach for bicyclic acetal thiolactams **4**-**9**.

Specifically, ester thiolactams **1**-**3** were prepared in good yields starting from the corresponding bicyclic lactams **I**-**III** by treatment with Lawesson's reagent in dry toluene.[23] Taking advantage of the increased reactivity of the ester moiety at C-7 carbon atom,[24] subsequent direct aminolysis under neat conditions gave the corresponding amide thiolactams **4**-**9** after overnight reaction at 45 °C. Contrary to the reactivity of bicyclic ester lactams, the reaction of ester thiolactams **1**-**3** with primary amines resulted in product degradation, possibly by ring opening of the thiolactam ring.

**Enzyme inhibition assays.** The screening of compounds **1**-**21** (Table 2) at 10 μM conc. for enzyme inhibition was performed to evaluate the modulation of BACE1 inhibition by the stereochemical arrangement of the pharmacophoric elements of the bicyclic compounds, and the different location of the amino acid side-chain isostere. A fluorometric assay kit (SensoLyte® 520 β-Secretase Assay Kit, Anaspec, USA) employing the fluorescent substrate HiLyte Fluor™ 488-Glu-Val-Asn-Leu-Asp-Ala-Glu-Phe-Lys (QXL™ 520)-OH was used, with excitation and emission wavelengths of 490 and 520 nm, respectively. Inhibition data (Table 2) showed lower inhibition potency as compared to what observed for SAP2 and HIV protease, suggesting that BACE1 possesses significant structural differences in the catalytic site, such as the different spatial relationship between the flap region and the two DTG and DSG aspartic protease motifs, as previously observed.

Lead SAP2 inhibitors **10** and **11**, and the stereoisomers of **11** containing the leucinol appendage (cmpd **12**-**14**) showed poor inhibition, whereas lead HIV protease inhibitors **15** and **16** showed better profile, indicating good accomodation in the BACE1 catalytic site. Similarly to what observed in previous reports on inhibition data towards SAP2 and HIV protease,[14,17] compounds lacking the carbonyl/thiocarbonyl group showed no inhibition (Table 2, **21**). Compound **4**, possessing a C=S bond, proved to be the most interesting inhibitor, and for this compound a dose-response measurement using 0.003-30 μM as the range of inhibitor concentrations was carried out, resulting in a $IC_{50}$ value of 2.6 μM (Figure 3).

The presence of the C=S bond in the bicyclic scaffold proved to be relevant, as thioamides **1**-**8** showed some inhibition with respect to other scaffolds, although with different degree, suggesting a role of the sulfur atom in addressing the flap region as a hydrogen-bonding acceptor. The morfoline appendage proved beneficial (Table 2, compounds **1**, **4**, **7**), although contrasting results were achieved when changing the scaffold (see inhibition data for **4**-**6**, and for **5**, **6** compared to **8**, **9**), suggesting the importance of balancing contributions from such appendage, the scaffold type and the C=O/C=S bond. Impaired activity was observed as a function of the appendage at the nitrogen atom and at the acetal position 5 of the scaffold, too, as compounds **17**-**20** failed to show any inhibition. No significant correlation was evinced with respect to the stereochemistry, although scaffold B (Scheme 1) showed some preference, and the matched combination of the decoration of such scaffold and the presence of C=O/C=S bond contributed significantly to inhibition, too (see inhibition data for compounds **5**, **8**, **15** and **16**).

**Molecular Docking.** Autodock 4.0.1[25] was used to evaluate the binding energies of minimum-energy conformations of compound **4**. Best-scoring conformations were clustered and visually inspected for enzyme-ligand interactions. Specifically, hydrogen-bonds to side chain oxygen atoms of the catalytic aspartic acids (D93 and D289), the hydrophobic interactions in the S1/S1' pockets and hydrogen-bonding to the 'flap region' were taken into account.

Docking results of **4** showed this molecule addressing the S1 binding pocket, and the acetal bridge being oriented towards catalytic D93 and D289, as expected (Figure 4).

**Table 2.** Inhibition data at 10 μM conc. of selected bicyclic compounds with diverse scaffold decoration and stereochemistry.

| Cmpd | scaffold | % Inhib. | Cmpd | scaffold | % Inhib. | Cmpd | scaffold | % Inhib. |
|---|---|---|---|---|---|---|---|---|
| **1** | 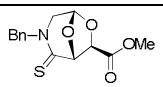 | 16 | **8** | 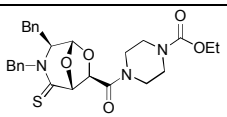 | 36 | **15** | 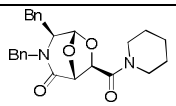 | 46 |
| **2** | 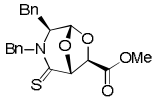 | 16 | **9** | 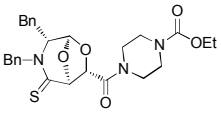 | 0 | **16** | 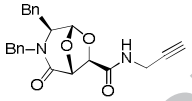 | 32 |
| **3** | 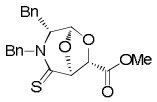 | 15 | **10** | 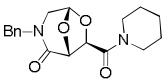 | 10 | **17** | 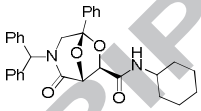 | 0 |
| **4** | 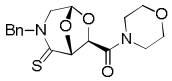 | **61** | **11** | 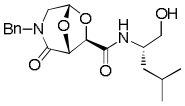 | 8 | **18** | 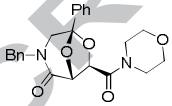 | 0 |
| **5** | 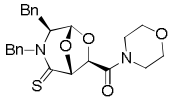 | 5 | **12** | 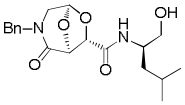 | 0 | **19** | 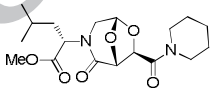 | 0 |
| **6** | 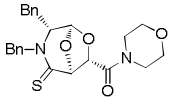 | 29 | **13** | 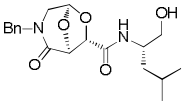 | 0 | **20** | 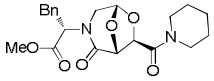 | 0 |
| **7** | 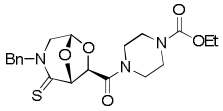 | 9 | **14** | 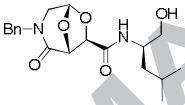 | 0 | **21** | 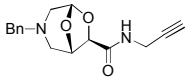 | 0 |

Interestingly, the global-minimum conformer was characterized by a hydrogen-bond between the thiocarbonyl group at position 2 of the scaffold and Q134 amide proton on the flap region of BACE1, confirming the typical binding orientation of these scaffolds within aspartic acid proteases. A π-stacking interactions between the *N*-benzyl group and F169/W176 side chains was observed as a key hydrophobic contact. The morpholine appendage proved to interact with R259 and Y189 establishing both polar and hydrophobic contacts. These results indicated the absence of interactions within S3 subsite, which are reported being essential for achieving high potency.[26]

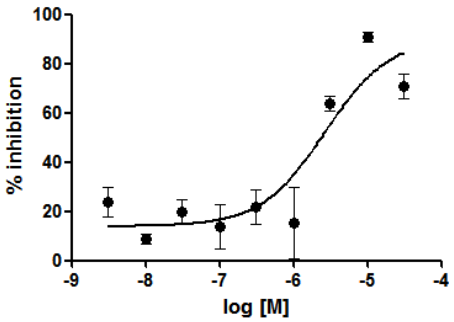


**Figure 3.** Percentage of inhibition of BACE1 activity by **4**, showing an $IC_{50}$ of 2.6±1.6 μM. Experiments were conducted in triplicate. Data are presented as means ± SD from three independent experiments.

## 3. Conclusions

BACE1 is the enzyme that initiates Aβ production by cleaving the extracellular domain of APP, and is recognised as a key therapeutic approach for reducing cerebral Aβ concentrations in patients with Alzheimer's disease.

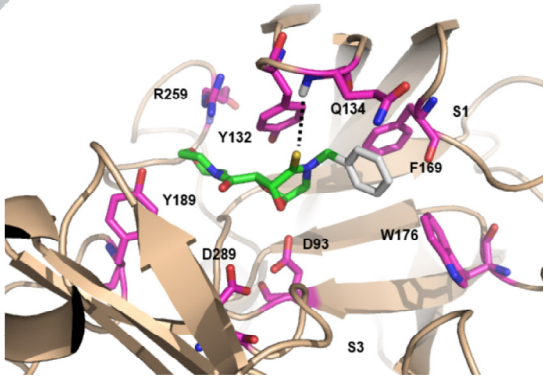


**Fig. 4** Compound **4** docked into the active site of BACE1 (PDB: 4J0P), highlighting protein residues (magenta) that form key interactions: D93/D289 vs acetal bridge, F169/W176 vs *N*-benzyl group, Q134 vs C=S bond, R259/Y189 vs morpholine group. Non-polar hydrogen atoms are omitted for clarity.

Taking advantage of a library of bicyclic molecular scaffolds possessing a bicyclic acetal portion as a potential transition-state analogue, which already showed activity towards other aspartic proteases such as SAP2 and HIV protease, we reasoned to test them towards BACE1 in enzyme inhibition kinetic assays. The analysis of the similarity of BACE1 with SAP2 from *C. albicans* and HIV-1 aspartic proteases was carried out by molecular modeling, and revealed a certain degree of structural analogy within the catalytic site, although the flap regions proved to be somewhat different in the three enzymes. Accordingly, a pool of amide thiolactams, aimed to target the BACE1 flap region more efficiently, were synthesized and assayed towards BACE1, thus allowing for the identification of compound **4** with potency in the

low micromolar range. Interestingly, other library members containing the C=O bond did not show similar potency as in previous studied aspartic proteases, confirming the existence of significant structural differences between these enzymes within the catalytic site.

Molecular docking calculations on compound **4** within BACE1 active site revealed an interesting binding mode, confirming the property of this scaffold in targeting the catalytic diad with the acetal moiety and interacting with the flap region through C=S hydrogen-bond. This compound will need further investigation and structure refinement in a hit-to-lead process in order to achieve promising BACE1 inhibitors based on novel molecular scaffolds. Specifically, potential toxicity issues of the thioamide bond will be studied, and chemical optimization will be be driven to improve bioactivity, without inhibiting the related aspartic protease cathepsin D, and with suitable *in vivo* profile for reducing cerebral Aβ concentrations in patients with Alzheimer's disease.

## 4. Experimental Section

### *4.1. General*

Analytical grade solvents and commercially available reagents were used without further purification. Reactions requiring an inert atmosphere were carried out under a nitrogen atmosphere. Dry toluene was distilled over Na/benzophenone. Flash column chromatography (FCC) purifications were performed using Merck silica gel (40-63 $\mu$m). TLC analyses were performed on Merck silica gel 60 F254 plates. $^{1}$H NMR spectra were recorded on a Varian Mercury 400 ($^{1}$H: 400 MHz),$^{13}$C spectra were recorded on a Varian Gemini 200 ($^{13}$C: 50 MHz). The chemical shifts (δ) and coupling constants (J) are expressed in parts per million (ppm) and hertz (Hz), respectively. Optical rotations were measured with JASCO DIP-360 digital polarimeter. Elemental analyses were recorded on a Perkin Elmer 240 CHN Analyzer. Mass spectra were carried out by direct inlet on a LCQ Fleet™ Ion Trap LC/MS system (Thermo Fisher Scientific) with an ESI interface in the positive mode.

### *4.2. General procedure for the synthesis of ester thiolactams **1-3***

The reaction was carried out on a scale of 0.2-0.6 mmol. An oven dried 25 mL round bottomed flask with two necks was equipped with a magnetic stir bar and charged with the Lawesson's reagent (0.5 eq). A 0.2 M solution of the corresponding bicyclic compound **I-III** (1 eq) in dry toluene was added to the Lawesson's reagent. The reaction mixture was refluxed for two hours, then the solvent was removed under reduced pressure and the crude product was purified by flash column chromatography.

### *4.3. Methyl (1S,5R,6R)-3-benzyl-4-thioxo-8-oxa-3-azabicyclo[3.2.1]octane-6-carboxylate (**1**)*

Purification by flash chromatography eluiting with 3:1 hexane-ethyl acetate (Rf 0.38) provided pure **1** as a brown solid with a yield of 65%. $[\alpha]_D^{23}$ = -74.4 (*c* 1.0, $CHCl_3$). $^{1}$H NMR (400 MHz, $CDCl_3$) δ 7.44-7.20 (m, 5H), 5.95 (d, *J* = 2.3 Hz, 1H), 5.50 (s, 1H), 5.14 (d, *J* = 2.6 Hz, 2H), 4.82 (s, 1H), 3.81 (s, 3H), 3.47 (dd, *J* = 13.5, 2.4 Hz, 1H), 3.25 (d, *J* = 13.5 Hz, 1H). $^{13}$C NMR (50 MHz, $CDCl_3$) δ 195.02, 168.83, 133.98, 128.87, 128.11, 127.83, 99.89, 82.92, 79.13, 77.80, 77.16, 76.52, 54.58, 53.37, 52.70. MS (ESI) m/z (%): 316.25 [$(M + Na)^+$, 100]. Anal. Calcd for $C_{14}H_{15}NO_4S$ (293.34): C, 57.32; H, 5.15; N, 4.77. Found: C, 57.72; H, 5.21; N, 4.68.

### *4.4. Methyl (1S,2S,5R,6R)-2,3-dibenzyl-4-thioxo-8-oxa-3-azabicyclo[3.2.1]octane-6-carboxylate (**2**)*

Purification by flash chromatography eluiting with 3:1 hexane-ethyl acetate (Rf 0.45) gave the pure product **2** as a yellow oil with a yield of 72%. $[\alpha]_D^{23}$ = -101.4 (*c* 1.0, $CHCl_3$). $^{1}$H NMR (400 MHz, $CDCl_3$) δ 7.49-7.16 (m, 8H), 7.06 (d, *J* = 7.7 Hz, 2H), 6.17 (d, *J* = 15.1 Hz, 1H), 5.62 (s, 1H), 5.50 (s, 1H), 4.79 (s, 1H), 4.48 (d, *J* = 15.1 Hz, 1H), 3.78 (s, 3H), 3.47 (dd, *J* = 10.8, 3.9 Hz, 1H), 3.23 (dd, *J* = 13.8, 3.9 Hz, 1H), 2.86 (dd, *J* = 13.7, 11.1 Hz, 1H). $^{13}$C NMR (50 MHz, $CDCl_3$) δ 195.53, 168.99, 135.26, 134.61, 129.15, 129.05, 128.23, 127.85, 127.64, 127.45, 101.17, 83.43, 79.90, 63.09, 52.84, 52.57, 36.53. MS (ESI) m/z (%): 406.17 [$(M + Na)^+$, 100]. Anal. Calcd for $C_{21}H_{21}NO_4S$ (383.46): C, 65.78; H, 5.52; N, 3.65. Found: C, 66.23; H, 5.79; N, 3.49.

### *4.5. Methyl (1R,2R,5S,6S)-2,3-dibenzyl-4-thioxo-8-oxa-3-azabicyclo[3.2.1]octane-6-carboxylate (**3**)*

Purification by flash chromatography eluiting with 3:1 hexane-ethyl acetate (Rf 0.45) to give the pure product **3** as a yellow oil with a yield of 69%. $[\alpha]_D^{23}$ = +102.2 (*c* 1.0, $CHCl_3$). $^{1}$H NMR (400 MHz, $CDCl_3$) δ 7.44-7.18 (m, 8H), 7.06 (d, *J* = 7.1 Hz, 2H), 6.17 (d, *J* = 15.1 Hz, 1H), 5.62 (s, 1H), 5.51 (s, 1H), 4.80 (s, 1H), 4.48 (d, *J* = 15.1 Hz, 1H), 3.78 (s, 3H), 3.46 (dd, *J* = 7.3, 3.2 Hz, 1H), 3.23 (dd, *J* = 13.8, 4.0 Hz, 1H), 2.85 (dd, *J* = 13.7, 11.0 Hz, 1H) $^{13}$C NMR (50 MHz, $CDCl_3$) δ 195.53, 168.99, 135.26, 134.61, 129.15, 129.05, 128.23, 127.85, 127.64, 127.45, 101.17, 83.43, 79.90, 63.09, 52.84, 52.57, 36.53. MS (ESI) m/z (%): 406.25 [$(M + Na)^+$, 100]. Anal. Calcd for $C_{21}H_{21}NO_4S$ (383.46): C, 65.78; H, 5.52; N, 3.65. Found: C, 66.11; H, 5.69; N, 3.51.

### *4.6. General procedure for the synthesis of amide thiolactams **4-9***

The reaction was carried out on a scale of 0.2-0.6 mmol. An oven dried 25 mL round bottomed flask was equipped with a magnetic stir bar and charged with the corresponding compound **1-3** (1 eq). The flask was cooled in an ice bath and the appropriate amine was added (10 eq). The reaction mixture was heated at 45 °C overnight. After adding ethyl acetate (40 mL), the organic phase was washed with 1 M HCl (3 x 15 mL), satd. $NaHCO_3$ solution (3 x 15 mL) and brine (1 x 20 mL). The organic phase was dried over $Na_2SO_4$, concentrated under a reduced pressure and the crude product was purified by flash chromatography.

### *4.7. (1R,5R,7R)-3-benzyl-7-(morpholin-4-ylcarbonyl)-6,8-dioxa-3-azabicyclo[3.2.1]octane-2-thione (**4**)*

Obtained from **1** using morpholine as the amine. Purification by flash chromatography eluiting with 2:3 hexane-ethyl acetate (Rf 0.41) gave the pure product **4** as a white solid with a yield of 71%. $[\alpha]_D^{23}$ = -36.9 (*c* 1.0, $CHCl_3$). $^{1}$H NMR (400 MHz, $CDCl_3$) δ 7.45-7.15 (m, 5H), 5.95 (d, *J* = 2.3 Hz, 1H), 5.53 (s, 1H), 5.21 (d, *J* = 14.5 Hz, 1H), 5.07 (d, *J* = 14.5 Hz, 1H), 4.97 (s, 1H), 3.79-3.55 (m, 8H), 3.49 (dd, *J* = 13.5, 2.4 Hz, 1H), 3.25 (d, *J* = 13.5 Hz, 1H). $^{13}$C NMR (50 MHz, $CDCl_3$) δ 196.08, 165.87, 134.14, 129.15, 128.43, 128.18, 99.96, 82.72, 79.36, 66.85, 66.61, 54.95, 53.69, 46.05, 42.72. MS (ESI) m/z (%): 371.22 [$(M + Na)^+$, 100]. Anal. Calcd for $C_{17}H_{20}N_2O_4S$ (348.42): C, 58.60; H, 5.79; N, 8.04. Found: C, 59.12; H, 5.98; N, 7.95.

### *4.8. (1R.4S,5R,7R)-3.4-dibenzyl-7-(morpholin-4-ylcarbonyl)-6,8-dioxa-3-azabicyclo[3.2.1]octane-2-thione (**5**)*

Obtained from **2** using morpholine as the amine. Purification by flash chromatography eluiting with 1:1 hexane-ethyl acetate (Rf 0.47) to give the pure product **5** as a colorless oil with a yield of 62%. $[\alpha]_D^{23}$= -78.2 (*c* 1.0, $CHCl_3$). $^{1}$H NMR (400 MHz,

$CDCl_3$) δ 7.46-7.14 (m, 8H), 7.05 (d, *J* = 7.5 Hz, 2H), 6.12 (d, *J* = 15.1 Hz, 1H), 5.63 (s, 1H), 5.50 (s, 1H), 4.94 (s, 1H), 4.53 (d, *J* = 15.1 Hz, 1H), 3.74-3.43 (m, 9H), 3.22 (dd, *J* = 13.8, 3.8 Hz, 1H), 2.87 (dd, *J* = 13.3, 11.4 Hz, 1H), $^{13}$C NMR (50 MHz, $CDCl_3$) δ 196.29, 165.93, 135.32, 134.73, 129.27, 129.22, 128.32, 127.74, 127.51, 101.12, 83.10, 80.07, 66.85, 66.60, 63.37, 52.69, 46.01, 42.67, 36.6. MS (ESI) m/z (%): 461.39 [(M + Na)$^+$, 100]. Anal. Calcd for $C_{24}H_{26}N_2O_4S$ (438.54): C, 65.73; H, 5.98; N, 6.39. Found: C, 65.99; H, 6.03; N, 6.31.

*4.9. (1S.4R,5S,7S)-3.4-dibenzyl-7-(morpholin-4-ylcarbonyl)-6,8-dioxa-3-azabicyclo[3.2.1]octane-2-thione (**6**)*

Obtained from **3** using morpholine as the amine. Purification by flash chromatography eluiting with 1:1 hexane-ethyl acetate (Rf 0.47) to give the pure product **6** as a colorless oil with a yield of 69%. $[\alpha]_D^{23}$ = +77.1 (*c* 1.0, $CHCl_3$). $^1$H NMR (200 MHz, $CDCl_3$) δ 7.58 – 7.26 (m, 8H), 7.06 ( d, J=7.5 Hz, 2H), 6.12 (d, *J* = 15.1 Hz, 1H), 5.63 (s, 1H), 5.50 (s, 1H), 4.94(s, 1H), 4.53 (d, *J* = 15.1 Hz, 1H), 3.74-3.43 ( m, 9H), 3.23 (dd, *J* = 13.8, 3.9 Hz, 1H), 2.87 (dd, *J* = 13.6, 11.1 Hz, 1H), $^{13}$C NMR (50 MHz, $CDCl_3$) δ 196.29, 165.93, 135.32, 134.73, 129.27, 129.22, 128.32, 127.74, 127.51, 101.12, 83.10, 80.07, 66.85, 66.60, 63.37, 52.69, 46.01, 42.67, 36.6. MS (ESI) m/z (%): 461.27 [(M + Na)$^+$, 100]. Anal. Calcd for $C_{24}H_{26}N_2O_4S$ (438.54): C, 65.73; H, 5.98; N, 6.39. Found: C, 65.97; H, 6.06; N, 6.18.

*4.10. Ethyl 4-{[(1R,5R,7R)-3-benzyl-2-thioxo-6,8-dioxa-3-azabicyclo[3.2.1]oct-7-yl]carbonyl}piperazine-1-carboxylate (**7**)*

Obtained from **1** using ethyl piperazine-1-carboxylate. Purification by flash chromatography eluiting with 1:1 hexane-ethyl acetate (Rf 0.23) to give the pure product **7** as a yellow solid with a yield of 61%. $[\alpha]_D^{23}$ = -41.5 (*c* 1.0, $CHCl_3$). $^1$H NMR (400 MHz, $CDCl_3$) δ 7.44-7.18 (m, 5H), 5.92 (s, 1H), 5.50 (s, 1H), 5.22 (d, *J* = 14.5 Hz, 1H), 5.04 (d, *J* = 14.5 Hz, 1H), 4.97 (s, 1H), 4.15 (q, *J* = 7.1 Hz, 2H), 3.72-3.42 (m, 9H), 3.24 (d, *J* = 13.5 Hz, 1H), 1.26 (t, *J* = 7.2 Hz, 3H) $^{13}$C NMR (50 MHz, $CDCl_3$) δ 195.93, 165.84, 155.34, 134.05, 129.07, 128.36, 128.12, 99.89, 82.54, 79.37, 77.79, 77.16, 76.52, 61.80, 54.85, 53.59, 45.24, 43.70, 43.38, 42.14, 14.68. MS (ESI) m/z (%): 442.31 [(M + Na)$^+$, 100]. Anal. Calcd for $C_{20}H_{25}N_3O_5S$ (419.49): C, 57.26; H, 6.01; N, 10.01. Found: C, 58.22; H, 6.10; N, 9.90.

*4.11. Ethyl 4-{[(1R.4S,5R,7R)-3.4-dibenzyl-2-thioxo-6,8-dioxa-3-azabicyclo[3.2.1]oct-7-yl]carbonyl}piperazine-1-carboxylate (**8**)*

Obtained from **2** using ethyl piperazine-1-carboxylate.Purification by flash chromatography eluiting with 1:1 hexane-ethyl acetate (Rf 0.36) to give the pure product **8** as a white solid with a yield of 65%. $[\alpha]_D^{23}$ = -51.0 (*c* 1.0, $CHCl_3$). $^1$H NMR (400 MHz, $CDCl_3$) δ 7.45-7.17 (m, 8H), 7.06 (d, *J* = 6.9 Hz, 2H), 6.12 (d, *J* = 15.1 Hz, 1H), 5.62 (s, 1H), 5.51 (s, 1H), 4.95 (d, *J* = 5.2 Hz, 1H), 4.16 (q, *J* = 7.0 Hz, 2H), 3.71-3.30 (m, 9H), 3.23 (dd, *J* = 13.8, 3.9 Hz, 1H), 2.87 (dd, *J* = 13.7, 11.1 Hz, 1H), 1.27 (t, *J* = 7.0 Hz, 3H), $^{13}$C NMR (50 MHz, $CDCl_3$) δ 196.29, 166.04, 155.46, 135.33, 134.75, 129.26, 129.13, 128.38, 128.04, 127.79, 127.56, 101.16, 83.09, 80.20, 63.39, 61.93, 52.74, 45.32, 43.82, 43.50, 42.25, 36.73, 14.77. MS (ESI) m/z (%): 532.03 [(M + Na)$^+$, 100]. Anal. Calcd for $C_{27}H_{31}N_3O_5S$ (509.62): C, 63.63; H, 6.13; N, 8.25. Found: C, 64.01; H, 6.28; N, 8.01.

*4.12. Ethyl 4-{[(1S.4R,5S,7S)-3.4-dibenzyl-2-thioxo-6,8-dioxa-3-azabicyclo[3.2.1]oct-7-yl]carbonyl}piperazine-1-carboxylate (**9**)*

Obtained from **3** using ethyl piperazine-1-carboxylate. Purification by flash chromatography eluiting with 1:1 hexane-ethyl acetate (Rf 0.36) to give the pure product **9** as a white solid with a yield of 62%. $[\alpha]_D^{23}$ = +49.6 (*c* 1.0, $CHCl_3$). $^1$H NMR (400 MHz, $CDCl_3$) δ 7.43-7.17 (m, 8H), 7.05 (d, J=6.8 Hz, 1H), 6.10 (d, *J* = 15.1 Hz, 2H), 5.58 (s, 1H), 5.53 (s, 1H), 4.95 (s, 1H), 4.53 (d, *J* = 15.1 Hz, 1H), 4.14 (q, *J* = 7.1 Hz, 2H), 3.65-3.39 (m, 9H), 3.21 (dd, *J* = 13.8, 4.0 Hz, 1H), 2.85 (dd, *J* = 13.8, 11.0 Hz, 1H), 1.25 (t, *J* = 7.1 Hz, 3H) ), $^{13}$C NMR (50 MHz, $CDCl_3$) δ 196.29, 166.04, 155.46, 135.33, 134.75, 129.26, 129.13, 128.38, 128.04, 127.79, 127.56, 101.16, 83.09, 80.20, 63.39, 61.93, 52.74, 45.32, 43.82, 43.50, 42.25, 36.73, 14.77. MS (ESI) m/z (%): 532.34 [(M + Na)$^+$, 100]. Anal. Calcd for $C_{27}H_{31}N_3O_5S$ (509.62): C, 63.63; H, 6.13; N, 8.25. Found: C, 63.89; H, 6.23; N, 8.10.

*4.13. Enzymatic BACE1 Assay*

Primary BACE1 enzymatic activity was assessed using a fluorometric assay kit (SensoLyte® 520 β-Secretase Assay Kit, Anaspec, USA) employing the fluorescent substrate HiLyte Fluor™ 488-Glu-Val-Asn-Leu-Asp-Ala-Glu-Phe-Lys (QXL™ 520)-OH. All the measurements were performed in 96-well plates with a BMG labtech OptimaStar microplate reader. The inhibitors (10 μM) were pre-incubated with the BACE1 enzyme (1 μg/mL) for 10 minutes at 25 °C before starting the reaction by substrate addition. The fluorescence was monitored over 30 minutes ($\lambda_{ex}$ =490 nm, $\lambda_{em}$=520 nm) at 25 °C. The percentages of inhibition for the test compounds were determined through the equation (1-Vs/Vo)∗100, where Vs is the initial velocity in the presence of the inhibitor and Vo is the initial velocity of the unhibited reaction. The $IC_{50}$ values were obtained by dose-response measurements using 0.003-30 μM as the range of inhibitor concentrations. All the experiments were performed in triplicate and the collected data were analyzed using Graphpad 4.0 software package (Graphpad Prism, San Diego, CA).

*4.14. Tridimensional structural alignment*

The Swiss PDB viewer (SPDBV) program (4.0.1 version, Swiss Institute of Bioinformatics)[19,20] was used to superimpose the three dimensional (3D) structures of HIV-1 aspartic protease (PDB code: 4HLA) and Secreted aspartic protease 2 from *C. albicans* (PDB code: 1EAG) with BACE1 (PDB code: 4J0P). Alpha-carbon atoms of the highly conserved DTG motif (e.g. Asp93, Thr94 and Gly95 for BACE1) were initially superimposed using the "fit molecule from selection" option. Then, using the "improve fit" option, SPDBV was asked to minimize the root-mean square distance (RMSD) between the corresponding atoms using a least square algorithm. The calculation was extended to neighbors until the maximum number of aligned atoms with the lowest RMSD was obtained.

*4.15. Pairwise sequence alignment*

Primary sequences of BACE1 (PDB: 4J0P), HIV-1 (PDB: 4HLA) and SAP2 (PDB: 1EAG) aspartic proteases were retrieved from the PDB in FASTA format. EMBOSS matcher, EMBL-EBI,[21] was used to carry out local alignments of the two proteins, by identifying local similarities in the two protein sequence using an algorithm based on Bill Pearson's Lalign application, version 2.0u4 (Feb. 1996). EBLOSUM-62 substitution matrix was used and penalties of 14 and 4 were applied for gap opening and extension, respectively.

*4.16. Docking Calculations*

Automated docking studies were carried out using the Lamarckian Genetic Algorithm (LGA) as a search engine implemented in the Autodock 4.0.1 program.[25] The AutoDockTools 1.4.5 (ADT) graphical interface[27] was used to prepare BACE1 and inhibitor PDBQT files. Coordinates of compound **4** were generated using Spartan (version 5.147), and

then energy-minimized through the AM1 semi-empirical method to calculate the equilibrium geometry. The coordinates of BACE1 protease were retrieved from the Protein Data Bank (PDB code: 4J0P), and enzyme-inhibitor complex was unmerged for achieving the free enzyme structure. Water molecules were removed. Hydrogen atoms were added to the enzyme and ligands, Gasteiger charges were added and non-polar hydrogens were merged. Three-dimensional energy scoring grids of 0.375 Å resolution and 40 Å×40 Å×40 Å dimensions were computed. The center of the grid was set using the coordinated of one of the oxygen atoms of D289. A total of 50 runs with a maximum of 2500000 energy evaluations were carried out for each ligand, using the default parameters for LGA. Cluster analysis was performed on docked results using a root-mean-square (rms) tolerance of 1.5 Å. The analysis of the binding mode of the docked conformations was carried out using the Autodock plugin within PyMol software v0.99.[28]

## Acknowledgments

Fondazione Cassa di Risparmio di Firenze is acknowledged for the CRF grant (2015.0935) entitled 'Sviluppo di nuovi inibitori peptidomimetici di beta-secretasi 1 (BACE-1) per il monitoraggio e trattamento di placche amiloidi nel morbo di Alzheimer'.

## References and notes

1. WHO (2012). Dementia, a Public Health Priority. Geneva: World Health Organization.
2. Wilmo, A.P.; Martin, P. *World Alzheimer Report 2010, The Global Economic Impact of Dementia.* London: Alzheimer's Disease International, 2010.
3. Selkoe, D.J. *Physiol. Rev.* **2001**, *81*, 741-766
4. Lee, V.M.; Balin, B.J.; Otvos, Jr, L.; Trojanowski, J.Q. *Science* **1991**, *251*, 675-678.
5. Vassar, R.; Kovacs, D.M.; Yan, R.; Wong, P.C. *J. Neurosci.* **2009**, *29*, 12787-12794.
6. Sisodia, S.S.; St George-Hyslop, P.H. *Nat. Rev. Neurosci.* **2002**, *3*, 281-290.
7. Luo, Y.; Bolon, B.; Kahn, S.; Bennett, B.D.; Babu-Khan, S.; Denis, P.; Fan, W.; Kha, H.; Zhang, J.; Gong, Y.; Martin, L.; Louis, J.C.; Yan, Q.; Richards, W.G.; Citron, M.;Vassar, R. *Nat. Neurosci.* **2001**, *4*, 231-232.
8. Ghosh, A.K.; Osswald, H.L. *Chem. Soc. Rev.* **2014**, *43*, 6765-6813
9. John, V. *Curr. Top. Med. Chem.* **2006**, *6*, 569-578.
10. Butler, C.R.; Ogilvie, K.; Martinez-Alsina, L.; Barreiro, G.; Beck, E.M.; Nolan, C.E.; Atchison, K.; Benvenuti, E.; Buzon, L.; Doran, S.; Gonzales, C.; Helal, C.J.; Hou, X.; Hsu, M.H.; Johnson, E.F.; Lapham, K.; Lanyon, L.; Parris, K.; O'Neill, B.T.; Riddell, D.; Robshaw, A.; Vajdos, F.; Brodney, M.A. *J. Med. Chem.* **2017**, *60*, 386-402.
11. Mandal, M.; Wu, Y.; Misiaszek, J.; Li, G.; Buevich, A.; Caldwell, J.P.; Liu, X.; Mazzola, R.D.; Orth, P.; Strickland, C.; Voigt, J.; Wang, H.; Zhu, Z.; Chen, X.; Grzelak, M.; Hyde, L.A.; Kuvelkar, R.; Leach, P.T.; Terracina, G.; Zhang, L.; Zhang, Q.; Michener, M.S.; Smith, B.; Cox, K.; Grotz, D.; Favreau, L.; Mitra, K.; Kazakevich, I.; McKittrick, B.A.; Greenlee, W.; Kennedy, M.E.; Parker, E.M.; Cumming, J.N.; Stamford, A.W. *J. Med. Chem.* **2016**, *59*, 3231-3248 and ref. therein.
12. Guarna, A; Guidi, A.; Machetti, F.; Menchi, G.; Occhiato, E.G.; Scarpi, D.; Sisi, S.; Trabocchi, A. *J. Org. Chem.* **1999**, *64*, 7347-7364.
13. Trabocchi, A.; Menchi, G.; Guarna, F.; Machetti, F.; Scarpi, D.; Guarna, A. *Synlett* **2006**, 331-353.
14. Trabocchi, A.; Mannino, C.; Machetti, F.; De Bernardis, F.; Arancia, S.; Cauda, R.; Cassone, A., Guarna, A. *J. Med. Chem.* **2010**, *53*, 2502-2509.
15. Calugi, C.; Trabocchi, A.; De Bernardis, F.; Arancia, S.; Navarra, P.; Cauda, R.; Cassone, A.; Guarna, A. *Bioorg. Med. Chem.* **2012**, *20*, 7206-7213.
16. De Bernardis, F.; Arancia, S.; Tringali, G.; Greco, M. C.; Ragazzoni, E.; Calugi, C.; Trabocchi, A.; Sandini, S.; Graziani, S.; Cauda, R.; Cassone, A.; Guarna, A.; Navarra, P. *J. Pharm. Pharmacol.* **2014**, *66*, 1094-1101.
17. Calugi, C.; Guarna, A.; Trabocchi, A. *Eur. J. Med. Chem.* **2014**, *84*, 444-453.
18. Hong, L.; Koelsch, G.; Lin, X.; Wu, S.; Terzyan, S.; Ghosh, A.K.; Zhang, X.C.; Tang, J. *Science* **2000**, *290*, 150-153.
19. Guex, N.; Peitsch, M.C. *Electrophoresis* **1997**, *18*, 2714-2723.
20. ExPAsy Proteomics Server. http://www.expasy.org
21. Calugi, C.; Guarna, A.; Trabocchi, A. *J. Enzyme Inhib. Med. Chem.* **2013**, *28*, 936-943.
22. EMBOSS Matcher - Pairwise Sequence Alignment from the EMBL-EBI tools website. http://www.ebi.ac.uk/Tools/psa/emboss_matcher/
23. Pederson, B.S.; Sheibye, S.; Nilsson, N.H.; Lawesson, S.-O. *Bull. Soc. Chim. Belg.* **1978**, *87*, 223-228.
24. Machetti, F.; Bucelli, I.; Indiani, G.; Kappe, C.O.; Guarna, A. *J. Comb. Chem.* **2007**, *9*, 454-461.
25. Morris, G.M.; Goodsell, D.S.; Halliday, R.S.; Huey, R.; Hart, W.E.; Belew, R.K.; Olson, A.J. *J. Comput. Chem.* **1998**, *19*, 1639-1662.
26. See, for example: Rombouts, F.J.; Tresadern, G.; Delgado, O.; Martínez-Lamenca, C.; Van Gool, M.; García-Molina, A.; Alonso de Diego, S.A.; Oehlrich, D.; Prokopcova, H.; Alonso, J.M.; Austin, N.; Borghys, H.; Van Brandt, S.; Surkyn, M.; De Cleyn, M.; Vos, A.; Alexander, R.; Macdonald, G.; Moechars, D.; Gijsen, H.; Trabanco, A.A. *J. Med. Chem.* **2015**, *58*, 8216-8235.
27. Gillet, A.; Sanner, M.; Stoffler, D.; Olson, A. *Structure* **2005**, *13*, 483-491.
28. DeLano, W.L. 'The PyMOL Molecular Graphics System.' DeLano Scientific LLC, San Carlos, CA, USA [http://www.pymol.org].

## Supplementary data

Supplementary data associated with this article can be found, in the online version, at http://dx.doi.org/10.1016